Supplementary Information

Supplementary Materials and Methods

Preparation and characterization of Muse and non-Muse cells

- *Culture of human bone marrow (BM)-derived mesenchymal stem cells (MSCs)*

Human BM-MSCs were purchased from Lonza (catalogue number: PT-2501, Lonza, Basel, Switzerland). Cells were cultured in α-minimum Essential Medium Eagle Modified (α-MEM) (Sigma-Aldrich, St. Louis, MO) with 10% fetal bovine serum (FBS) and 0.1 mg/ml kanamycin sulfate (Invitrogen, Carlsbad, CA) at 37°C in 95% air and 5% CO_2. Cells from passages 4 through 8 were used for Muse and non-Muse isolation.

- *Isolation of human Muse and non-Muse cells*

Human Muse and non-Muse cells were isolated by fluorescence-activated cell sorting (FACS) as described previously.[1] Briefly, BM-MSCs were incubated with rat anti-SSEA-3 antibody (1:100; Millipore, Billerica, MA) for 1 h on ice and labeled with fluorescein isothiocyanate (FITC)-conjugated anti-rat IgM (1:100; Jackson ImmunoResearch, West Grove, PA). Muse cells were obtained as the SSEA-3(+) population and non-Muse cells as the SSEA-3(-) population using FACS AriaII (Becton Dickinson, Franklin Lakes, NJ).

For labeling with green fluorescent protein (GFP), BM-MSCs were infected with GFP-lentivirus, as previously described.[2,3] Lentiviral vectors pMD2G, pCMV deltaR8.74, and pWPXL were kindly provided by Dr. D. Trono (Laboratory of Virology and Genetics, EPFL, Switzerland).[2] In brief, the plasmids were transfected into LentiX-293T packaging cells (Takara Bio Inc, Shiga, Japan) using Lipofectamine 2000 (Thermo Fisher Scientific, MA). The viral supernatant was collected 3 d later, centrifuged, and filtered through a 0.45-μm filter. The transduction efficiency evaluated by FACS was ~70%.

To obtain GFP-labeled Muse and non-Muse cells, BM-MSCs introduced with the GFP-lentivirus were incubated with rat anti-SSEA-3 IgM antibody (1:100; Millipore), detected by allophycocyanin-conjugated anti-rat IgM (Jackson Immunoresearch, West Grove, PA) in the antibody diluents, and sorted by Special Order Research Products FACSAriaII (Becton Dickinson) as described previously,[1] using a 488-nm blue laser for sorting GFP(+) cells and a 633-nm red laser for separating the SSEA-3(+) and (-) cell populations.

- *Single-suspension culture and triploblastic differentiation*

Isolated Muse cells were confirmed to be stress-tolerant against long-term trypsin incubation for ~16 h, as described previously (data not shown).[1] To further confirm the pluripotent properties of Muse cells, Muse and non-Muse cells were separated by cell sorting as described above and subjected to single-cell suspension culture after limiting dilution, as described previously.[1] Ten days

later, each single cell-derived cluster was individually picked up and plated onto gelatin-coated plates, and then the clusters were allowed to expand cells in α-MEM with 10% FBS, 1% kanamycin, and 2 mM L-glutamine. After 2 wk, the expanded cells were stained with neurofilament (1:200; Millipore), α-smooth muscle actin (1:100; Abcam, Cambridge, UK), and cytokeratin 7 (1:100; Millipore).

Gene expression of Muse cells and non-Muse cells

Isolated GFP(+) Muse and non-Muse cells were cultured overnight in adherent culture in 10% FBS/α-MEM containing 2 mM L-glutamine and 0.1 mg/ml kanamycin. RNA was then extracted using Nucleo RNA SpinXS (Macherey-Nagel, Düren, Germany) according to the manufacturer's protocol, followed by cDNA synthesis using Super Script VILO (Invitrogen). Gene expression of *Oct3/4*, *Nanog*, *Sox2*, and *β-actin* were determined by quantitative-PCR (Q-PCR) with 2× Taqman Universal Master Mix II with UNG (Life Technologies, Carlsbad, CA) and Taqman probes (Oct3/4, Hs01895061u1; Nanog, Hs02387400g1; Sox2, Hs01053049s1; β-actin, Hs01060665g1) on 7500 Fast Real-time PCR systems (Applied Biosystems, Foster City, CA). The expression levels of *Oct3/4*, *Nanog*, and *Sox2* were normalized to *β-actin*. Each Q-PCR reaction was run in triplicate in separate wells.

In vitro differentiation of Muse cells into renal lineage

A renal-lineage differentiation study was conducted according to the method reported by Batchelder et al[4]. Muse and non-Muse cells (1×10^4 each) were incubated in α-MEM containing 10% FBS, 0.1 mg/ml kanamycin, 2 mM L-glutamine, and 100 μM β-mercaptoethanol on poly 2-hydroxyethyl methacrylate (poly-HEMA; Sigma-Aldrich) -coated dishes for 2 d. After 2 d in suspension culture, Muse and non-Muse cells were plated on gelatin-coated 24-well dishes and cultured in 10% FBS/DMEM including 0.1 mg/ml kanamycin, 0.1 μM all-trans retinoic acid (Sigma-Aldrich), 10 ng/ml activin-A (Wako, Tokyo, Japan), and 50 ng/ml recombinant human bone morphologic protein-7 (Wako). After 3 wk of adherent culture, total RNA was extracted using NucleoSpin RNA XS, and then cDNA was synthesized using Superscript VILO. Q-PCR was performed with 2× SYBR Green Master Mix (Life Technologies, Carlsbad, CA) according to the manufacturer's instructions. Human fetus kidney total RNA as a positive control for Q-PCR was obtained from Takara Bio Inc (#Z6584N, Takara Bio Inc, Shiga, Japan).

The expression levels of *WT1* and *EYA1* were normalized to glyceraldehyde-3-phosphate dehydrogenase (GAPDH). The sequences of the *WT1*, *EYA1*, and *GAPDH* primers were as follows: *WT1* forward, 5'- CTTCAGAGGCATTCAGGATGTG -3'; reverse, 5'- TCTCAGATGCCGACCGTACA-3'. *EYA1* forward, 5'- GATGTCAAGTGTCAGTAAGGAT-3'; reverse, 5'- AAGTGAGGTGGTAGGAGAG -3'. *GAPDH* forward, 5'-

CTTCGCTCTCTGCTCCTCCT -3'; reverse, 5'- GTTAAAAGCAGCCCTGGTGA -3'. Each reaction was run in triplicate. Three samples were evaluated for the Muse and non-Muse cells.

Focal segmental glomerulosclerosis (FSGS) model and transplantation

All animal experiments were approved by Tohoku University's Bioethics Committee. Male severe combined immunodeficiency (SCID; CB17/Icr-Prkdc<scid>/CrlCrlj) mice (8 wk old) and male BALB/c (BALB/cCrSlc) mice (8 wk old) were purchased and maintained in a specific pathogen-free environment at the animal facilities of Tohoku University Graduate School of Medicine. They were maintained under 12-h light/dark conditions with free access to water and diet. Before making the FSGS model, blood and 16-h urine samples were collected from each animal. Blood was collected from the tail vein, and urine was collected using metabolic cages with free access to water and a gelled diet to avoid contamination of the urine sample with feed. Blood urea nitrogen (BUN) was measured using an auto-analyzer (DRI-CHEM 2000V, Fuji Film, Tokyo, Japan). Plasma and urine creatinine were measured using the modified Jaffe's method (BioAssay Systems, Hayward, CA) and urine protein was determined by the Bradford method (Bio-Rad Laboratories, Hercules, CA). Creatinine clearance was calculated as follows: Creatinine clearance (μl/min) = [urine creatinine concentration (mg/dl) × urine volume (μl/min) / plasma creatinine concentration (mg/dl)]. After obtaining the basic urine protein creatinine ratio, creatinine clearance, plasma creatinine, and BUN values, FSGS was induced by tail vein injection of doxorubicin hydrochloride (DOX; Wako, Osaka, Japan) at a concentration of 5.3 mg/kg body weight for SCID mice (11-14 wk old) and 11.5 mg/kg body weight for BALB/c mice (11-14 wk old). One week after DOX administration, the SCID and BALB/c mice were each divided into three groups: Muse, non-Muse, and vehicle groups. The Muse and non-Muse groups received an injection of 2×10^4 Muse cells or non-Muse cells suspended in sterile saline, respectively, via the tail vein, and the vehicle group received an equivalent volume of sterile saline. In the SCID mouse experiment, 9 mice were allocated to each of the Muse and non-Muse groups and 10 mice were allocated to the vehicle group. In the BALB/c mouse experiment, 5 mice were allocated to each group. Urine protein creatinine ratio, creatinine clearance, plasma creatinine, and BUN levels were measured before DOX injection, and at 7 wk after cell infusion in the SCID mice, and at 5 and 7 wk in the BALB/c mice.

For immunohistochemistry, 2×10^4 GFP-labeled Muse or GFP-labeled non-Muse cells were infused via the tail vein into FSGS-SCID mice and FSGS-BALB/c mice. GFP-labeled Muse or non-Muse cell-infused FSGS-SCID mice (n=3/group) were fixed at 7 wk. GFP-labeled Muse or non-Muse cell-infused FSGS-BALB/c mice (n=3/group) were fixed at 5 wk.

For *in vivo* dynamics, GFP(+) cells in every organ were counted using the A1 confocal microscope with a spectral unmixing system (Nikon, Tokyo, Japan), and the GFP signal was extracted from the autofluorescence. Approximately 30 randomly selected areas were counted. Three

FSGS-SCID mice were prepared for each group at each time-point (intact, 2 and 7 wk after cell infusion). Cell number was expressed as GFP(+) cells per mm^2, and the mean ± SE was calculated.

For terminal deoxynucleotidyl transferase dUTP nick end labeling (TUNEL), PCNA and Ki67 staining in podocytes (podocin- and WT1-positive) and endothelial cells (CD31-positive), 2×10^4 GFP-labeled Muse or non-Muse cells were infused via the tail vein into FSGS-BALB/c mice and were evaluated at 3 d, 10 d, and 5 wk after cell infusion (n=3 for each group).

Immunohistochemistry

Animals were deeply anesthetized, transcardially perfused with periodate-lysin-paraformaldehyde fixate, and the kidney and other organs (i.e., brain, lung, heart, liver, spleen, muscle) were dissected out. Samples were frozen in Optimal Cutting Temperature compound or embedded in paraffin. First, cryosections (6-7 μm thick) were incubated with 1% sodium dodecyl sulfate in phosphate buffered saline (PBS) for antigen retrieval for 5 min, and with blocking solution containing 5% bovine serum albumin for 30 min at room temperature (RT). Sections were then incubated with rabbit anti-58K Golgi protein antibody (anti-human Golgi complex antibody, 1:300; Abcam), which reacts only with human cells (not with SCID or BALB/c mouse cells), or goat anti-GFP antibody (1:1000; Abcam) at 4°C overnight to detect human Muse and non-Muse cells. For glomerular cell markers, the following antibodies were used: WT1 (1:200; Santa Cruz Biotechnology, Dallas, TX), podocin (1:300; Abcam), megsin (1:200; Bioss, Woburn, MA), CD31 (1:200; Santa Cruz Biotechnology), and von Willebrand factor (1:1000; DAKO). For the cell proliferation marker, Ki67 (1:100; Thermo Fisher Scientific, MA, USA) or PCNA (1:500; Abcam) was used. For the immune cell marker, CD45 (1:50; BD Pharmingen, San Diego, CA) and F4/80 (1:100; AbD Serotec Ltd., Oxford, UK) were used. After overnight incubation with primary antibodies, sections were incubated with the appropriate secondary antibodies for 2 h at RT as follows: anti-rabbit IgG antibody conjugated with Alexa Fluor 488 (1:500; Jackson Immunoresearch) was used for anti-human Golgi complex antibody; anti-goat IgG antibody conjugated with Alexa Fluor 488 (1:500; Jackson Immunoresearch) was used for the anti-GFP antibody; anti-goat IgG antibody conjugated with Alexa Fluor 594 (1:500; Jackson Immunoresearch) was used for the anti-GFP antibody for the spectral unmixing system in the laser confocal microscopy; anti-rabbit IgG antibody conjugated with Alexa Fluor 568 (1:500; Life Technologies) was used for the anti-WT1 antibody, anti-podocin antibody, anti-megsin antibody, and anti-von Willebrand factor antibody; anti-rabbit IgG-Alexa Fluor 647 was used for the anti-WT1 antibody and Ki67; anti-goat IgG antibody conjugated with Alexa Fluor 680 (1:500; Life Technologies) was used for anti-CD31 antibody; anti-mouse IgG antibody conjugated with Alexa Fluor 568 (1:500; Life Technologies) was used for anti-CD45 antibody and anti-PCNA; and anti-rat IgG antibody conjugated with Alexa Fluor 568 (1:500; Life Technologies) was used for the anti-F4/80 antibody. Rhodamine-labeled wheat germ agglutinin (WGA) was used at 1:500

(Vectastain, Burlingame, CA). Sections were then stained with 4',6-diamidino-2-phenylindole and washed five times with PBS. Samples were mounted and observed under a confocal laser microscope (Nikon, Tokyo, Japan).

The ratio of glomerular cell differentiation in Muse cells was determined based on the co-localization of each renal cell-marker with GFP- or human Golgi complex-positive cells in 30 glomeruli from each of 3 double-stained sections. The data from three animals for each experiment were used to calculate the mean ± SE.

Human genome detection from murine kidney

DNA was extracted from the murine kidney as well as other organs in each group (2 samples) using a REDExtract-N-Amp Tissue PCR kit (Sigma-Aldrich) with the modified protocol previously described by Alcoser et al.[5] Extracted DNA was diluted in Tris-EDTA buffer, and the concentration was determined by NanoDrop 1000 3.6.0. (Thermo Fisher Scientific). Human Alu sequence-specific Q-PCR was performed (n=3/sample) with 100 ng of DNA, 2× Taq Man Universal Master Mix II with UNG (Applied Biosystems), primers, and probe (forward PCR primer, 5' -CATGGT-GAAACCCCGTCTCTA-3'; reverse, PCR primer, 5'-GGGTTCAAGCGATTCTCCTG-3'; TaqMan probe, 5'-FAM-ATTAGCCGGGCGTGGTGGCG-TAMRA-3) on a 7500 Fast Real-time PCR system (Applied Biosystems). We obtained a standard curve by using samples in which human and murine genomes were mixed, as described in our previous report.[6] The amount of human genome in the kidney of each group was calculated by applying the Ct value obtained for each sample to the standard curve.[6]

Migration assay

The migration assay using a Matrigel invasion chamber (Becton Dickinson) was performed according to the manufacturer's protocol. Briefly, serum was collected from either FSGS-SCID that was injected with DOX 1 wk before, or normal SCID mice (DOX was not injected). To assay the migration toward serum, the lower chamber was filled with α-MEM containing 20% of the serum collected from FSGS-SCID or normal SCID mice. For the control, serum-free α-MEM was used. Immediately after, 3.5×10^4 Muse or non-Muse cells suspended in serum-free α-MEM were placed in the upper chambers, and the wells were incubated at 37°C, 5% CO2 for 22 h. The migrated cells were then fixed and stained with the Diff-Quik kit (Becton Dickinson). The number of migrated cells was calculated under a light microscope at 200× magnification in three random fields for each well. The experiment was repeated three times.

To assess the migration ability of Muse cells through the glomerular basement membrane, a CytoSelect 24-well Cell Invasion Assay, Colorimetric (Cell Biolabs Inc., San Diego, CA, CBA-110)

was used. The upper surface of the microporous membrane located between the upper and lower chambers was coated with a uniform layer of basement membrane matrix (Cell Biolabs). Muse cells in serum-free media were placed in the upper chamber, and a tissue slice of FSGS-SCID kidney was placed in the lower chamber. For the control, serum-free medium was placed in the lower chamber. The number of Muse cells that migrated into the lower chamber through the basement membrane was calculated at 24 h after starting the incubation.

FISH

FISH was performed according to the manufacturer's protocol. Frozen tissue sections (10 μm thick) were fixed with 4% paraformaldehyde/PBS for 30 min at 4°C. They were washed in PBS, and treated with 0.1% pepsin (Wako, Osaka, Japan)/0.1M HCl for 6 min at 37°C. The slides were dehydrated with a graduated ethanol series (70%, 85%, and 100% ethanol) for 2 min each at RT and air dried. The mixtures of human genomic DNA-specific probe (SPH-20, Chromosome Science Labo Ltd., Sapporo, Japan) labeled with Red-dUTP (Abbott Molecular Probes, Abbott Park, IL) and mouse genomic DNA-specific probe (SPM-20, Chromosome Science Labo Ltd.) labeled with Green-dUTP (Abbott Molecular Probes) were added to the slides. Sections were denatured for 10 min at 80°C, and hybridized overnight at 37°C. The next day, the sections were washed with 2× SSC (saline sodium citrate) for 5 min at 37°C. They were washed with 50% formamide/2× SSC for 20 min at 37°C, with 1× SSC for 15 min at RT, and then counterstained with DAPI. These images were compared with the corresponding fluorescence images of neighboring sections stained with GFP and WT1. Fusion frequency was determined for 50 human chromosome(+) cells in each of 3 sections.

PAS and Masson-trichrome staining

Paraffin sections (3 μm thick) were used. For analysis of glomerular sclerosis, the PAS-positive area/glomerular area was determined by evaluating 20 glomeruli per section under a light-microscope with imaging software (NIS Elements, Nikon, Japan). To evaluate interstitial fibrosis, 10 non-overlapping fields from the cortical area were observed in each section stained with Masson-trichrome. The fibrotic area per one optical field was measured using the same device (NIS Elements). Five animals for each group in the SCID experiment and three animals for each group in the BALB/c experiment were analyzed.

TUNEL

For TUNEL staining, an In Situ Cell Death Detection Kit, TMR Red (Roche Diagnostics, Basel, Switzerland) was used according to the manufacturer’s instructions. Briefly, cryosections were treated with freshly prepared 1% sodium dodecyl sulfate for 5 min at RT, washed with PBS, treated with immunohistochemistry against CD31 and podocin, and visualized using secondary antibodies

labeled with Alexa Fluor 647 (see Immunohistochemistry section). After immunohistochemical staining, the sections were further incubated with the TUNEL reaction mixture containing the Enzyme Solution and Label Solution (1:9) for 1 h at 37ºC in a humidified chamber, and finally washed in PBS. For the negative TUNEL staining control, the Label Solution was used instead of the TUNEL reaction mixture.

Indoleamine 2, 3 dioxygenase (IDO) activity assay, and Western blot

An IDO activity assay was performed according to a previous study,[7] with modification. Muse and non-Muse cells were separately plated on 6-well culture plates (final cell density: 1×10^4 cells/cm^2) and cultured in regular culture medium with 50 ng/ml of interferon-gamma (Wako, Osaka, Japan) for 72 h.

The expression of IDO and β-actin was assessed by Western blot analysis. Muse and non-Muse cells were washed with PBS and scraped into lysis buffer (20 mM Tris-HCl [pH7.5], 150 mM NaCl, 1% Triton X-100) containing complete protease inhibitor (Roche Diagnostics). Ten micrograms of denatured protein samples was loaded and separated on 10% sodium dodecyl sulfate-polyacrylamide gels and transferred onto a polyvinylidene difluoride membrane (Millipore). The blots were blocked in 5% skim milk (Nacalai Tesque, Kyoto, Japan) in Tris-buffered saline with 0.05% Tween 20, incubated with the primary antibodies: rabbit monoclonal anti-IDO antibody (ab76157, 1:10,000, Abcam) or mouse monoclonal anti-β-actin antibody (ab6276, 1:10,000, Abcam) overnight at 4ºC, followed by incubation with the appropriate secondary antibodies: donkey anti-rabbit IgG antibody conjugated to HRP (1:5000, Jackson ImmunoResearch) or goat anti-mouse IgG antibody conjugated to HRP (1:5000, Jackson ImmunoResearch). The signals were visualized with Pierce ECL Plus Western Blotting Substrate (Thermo Fisher Scientific) and detected by a lumino image analyzer (LAS-4000 mini, Fuji Film).

Mixed lymphocyte proliferation assay

The effect of Muse and non-Muse cells on the proliferation of human peripheral blood mononuclear cells (PBMCs) was assessed. PBMCs were obtained from Lonza (Cat# CC-2702, Lot# 0000540101), labeled with 1 mM 5-(and-6)-carboxyfluorescein diacetate succinimidyl ester (Vybrant CFDA-SE Cell Tracer kit, Thermo Fisher Scientific), and treated with Dynabeads Human T-Activator CD3/CD28 (Thermo Fisher Scientific). Muse and non-Muse cells were plated onto a 24-well culture plate (final cell density: 2×10^4 cells/cm^2) and co-cultured with PBMCs (final cell density: 5×10^5 cells/cm^2) in RPMI1640 with 2 mM L-glutamine, 1 mM sodium pyruvate, 0.1 mg/ml kanamycin, and 10% FBS. PBMCs were corrected and analyzed by flow cytometry (FACS AriaII, Becton Dickinson). The proliferation rate was calculated according to the manufacturer's instructions.

Q-PCR for renoprotective factors

Total RNA extracted from the kidney of the Muse, non-Muse, and vehicle groups (n=5/group) at 2 wk was purified using RNeasy Mini Kit (QIAGEN). First-strand cDNA was generated using Oligo$(dT)_{20}$ primers and SuperScript III reverse transcriptase. cDNA was amplified using the Applied Biosystems 7500 fast real-time PCR systems according to the manufacturer's instructions. Mouse-specific primers for hepatocyte growth factor (Mm01135185_m1), vascular endothelial growth factor A (VEGF-A) (Mm00437306_m1), VEGF-B (Mm00442100_g1), VEGF-C (Mm00437310_m1), VEGF-D (Mm01131929_m1), epidermal growth factor (EGF) (Mm00438696_m1), insulin-like growth factor-1 (IGF-1) (Mm00439560_m1), transforming growth factor alpha (TGF-alpha) (Mm00435858_m1), and beta-actin (Mm02619580_g1) were obtained from Applied Biosystems. Data were processed using the ΔΔCt method. To compare the results of all the experiments, the vehicle Ct value was set as a gene expression level of 1.

Statistics

Group comparisons of renal function were performed using repeated measures analysis of variance (ANOVA) followed by the Bonferroni multiple-comparison correction. The group comparisons of pre-DOX vs 5 wk after DOX and of 5 wk vs 7 wk after DOX in SCID mice were performed using factorial ANOVA followed by the Bonferroni correction. Group comparisons of pathologic parameters were performed using a one-way ANOVA, followed by the Bonferroni correction. The migration assay was analyzed by one-way ANOVA, followed by the Bonferroni correction. The difference in the integrated cell number between the Muse and non-Muse groups was analyzed using a t-test. A p-value <0.05 was considered statistically significant. Data are shown as mean±SE.

Supplementary Results

Supplementary Result 1

Percentage of Muse cells after passages

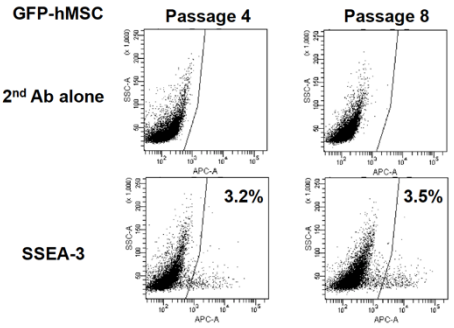

The percentage of Muse cells did not largely change, even between the 4th and 8th passages of human GFP(+) MSCs.

Supplementary Result 2

Distribution of systemically administered Muse cells

1) Q-PCR for human-specific DNA Alu sequence

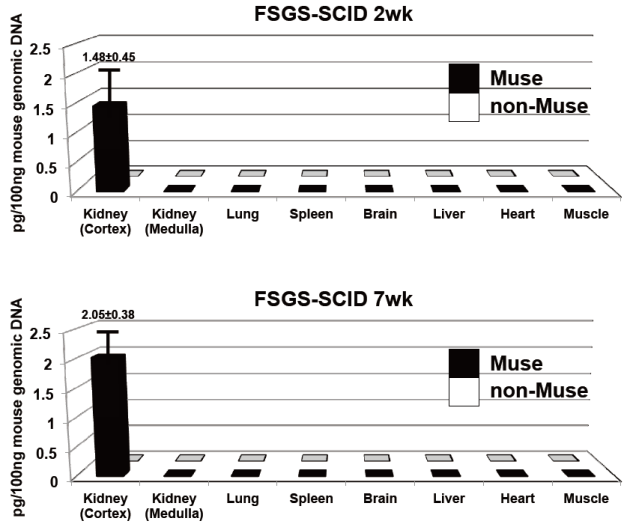

Detection of the Alu sequence in the Muse and non-Muse groups at 2 wk and 7 wk. The main target of doxorubicin in the kidney is the glomerulus.[8] Therefore, the main locus of Muse cell engraftment is considered to be the cortex and not the medulla. We split the kidney into the cortex and medulla, and separately subjected the tissues to Q-PCR. Consequently, the human Alu sequence was detected in the cortex of the kidney whereas in the tissues obtained from other organs, including the medulla of the kidney, the human Alu sequence was under the detection limits at both 2 wk and 7 wk.

2) GFP(+) Muse cells were detected in the cortex and medulla of the FSGS-SCID kidney under an

A1 confocal microscope equipped with a spectral unmixing system (Nikon, Tokyo, Japan) at 7 wk.

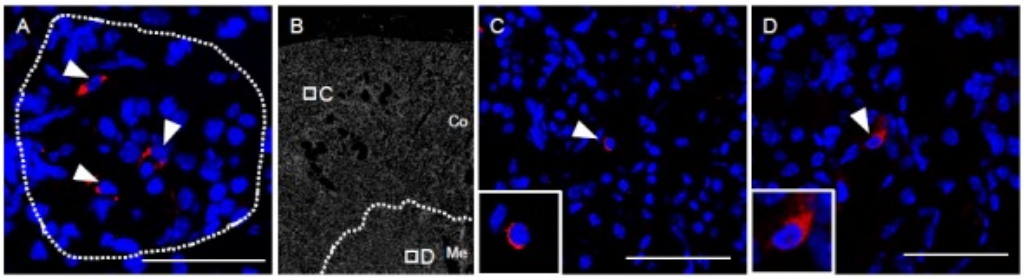

The GFP signal detected by Alexa Fluor 594 was extracted from autofluorescence using a spectral unmixing system in the laser confocal microscopy. (A) Example of GFP(+) Muse cells (arrowheads) in the glomerulus (dotted line). The majority of GFP(+) Muse cells were detected in the glomerulus. (B) Low power field of the cortex (Co) and medulla (Me) of the kidney. (C) In the cortex, a small number of GFP(+) Muse cells (arrowheads) were observed in areas other than glomerulus (corresponds to the square C in (B)). (D) A small number of GFP(+) Muse cells were also detected in the medulla (corresponds to the square D in (B)). Bars=50 μm.

Supplementary Result 3

The lung, heart, and liver of the Muse cell-infused FSGS-SCID mice at 7 wk

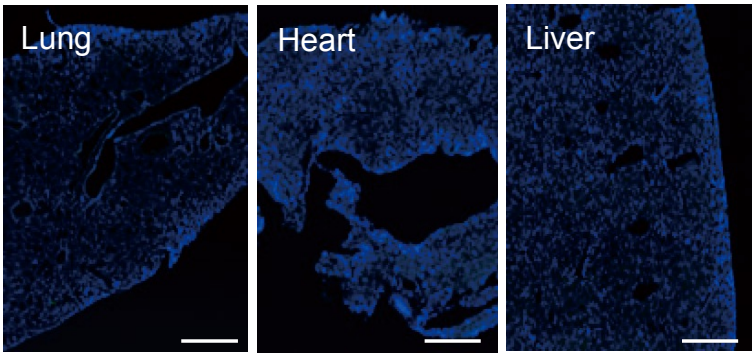

Bars= 1mm

GFP(+) Muse cells were not detectable in these organs in histologic samples.

Supplementary Result 4

Muse cell integration varied among glomeruli in the FSGS model

At the time of the infusion of the cells (7 d after DOX injection), the degree of damage among glomeruli varied considerably in the FSGS kidney. As shown below, some glomeruli showed severe damage in podocytes and endothelial cells, suggested by podocin and CD31 staining, respectively, whereas other glomeruli showed intermediate or only slight damage.

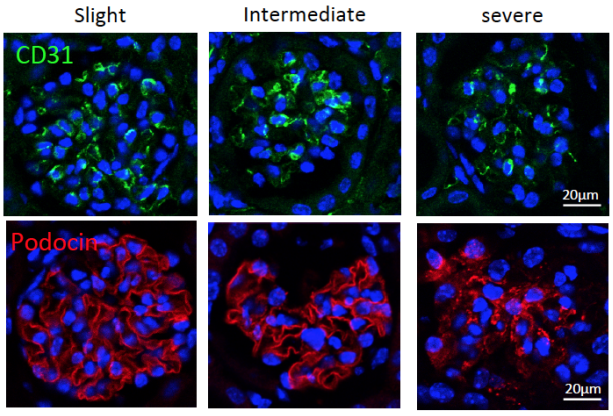

As reported in other models, such as muscle degeneration, hepatectomy, and liver cirrhosis,[9-11] Muse cells preferentially migrate to and integrate into the damaged site following systemic administration. In this context, Figure 11 in the main text shows that Muse cells actively migrated toward the serum of the FSGS model compared to that of normal mice *in vitro*. These results suggested that Muse cells preferentially integrated into the damaged glomeruli rather than intact- or slightly-damaged glomeruli, unless vessels in the glomerulus were not collapsed. This may partly explain why the degree of Muse cell integration varied among glomeruli at 7 wk as shown in Figure 2D.

In addition to counting GFP(+) cells/mm^2 (Figure 2B, C), we focused on GFP(+) cell-containing glomeruli in the Muse group-kidney and calculated the mean number of GFP(+) cells/glomerulus (confined only to GFP(+) cell-containing glomeruli) per section, which resulted in 3.20 ± 0.15 (mean ± SE) at 2 wk and 3.67 ± 0.64 at 7 wk, in FSGS-SCID, and 2.87±0.14 cells at 5 wk in FSGS-BALB/c. The mean ratio of glomeruli containing GFP(+) cells per total glomeruli per section was 8.5±0.3% in FSGS-SCID at 7 wk and 7.3±0.5% in FSGS-BALB/c at 5 wk.

The functional recovery and pathologic improvement in the Muse group is considered partly due to the differentiation of Muse cells, while the number of GFP(+) Muse cells per glomerulus (confined only to GFP(+) cell-containing glomeruli) per slice was ~4 cells in FSGS-SCID mice and ~3 cells in FSGS-BALB/c mice. In both FSGS-SCID and FSGS-BALB/c mice, ~30% of GFP(+)-Muse cells in the glomerulus expressed markers for podocytes, ~13% expressed markers for mesangial cells, and ~45% expressed markers for endothelial cells. Thus, we calculated that 1~1.2 podocytes, 0.4~0.5 mesangial cells, and 1.3~1.8 endothelial cells per glomerular section in a slice were provided by the Muse cells. In addition, the rate of glomeruli that contained GFP(+) cells was only 7.3%~8.5%, as mentioned above. It is thus difficult to conclude that functional recovery was delivered only by the differentiation of Muse cells into glomerular cells. Nevertheless, the recovery in renal function, represented by the creatinine clearance rate, in the Muse group, particularly in the Muse cell-infused FSGS-BALB/c mice, might be due not only to differentiation but also to synergistic effects of Muse cells, including paracrine (Supplementary Result 13),

immunomodulatory (Supplementary Result 10), and fibrolytic[6] effects. In addition to cell differentiation, these effects cooperatively delivered functional recovery in this model.

Supplementary Result 5

Single channel images used to produce Figure 2D.

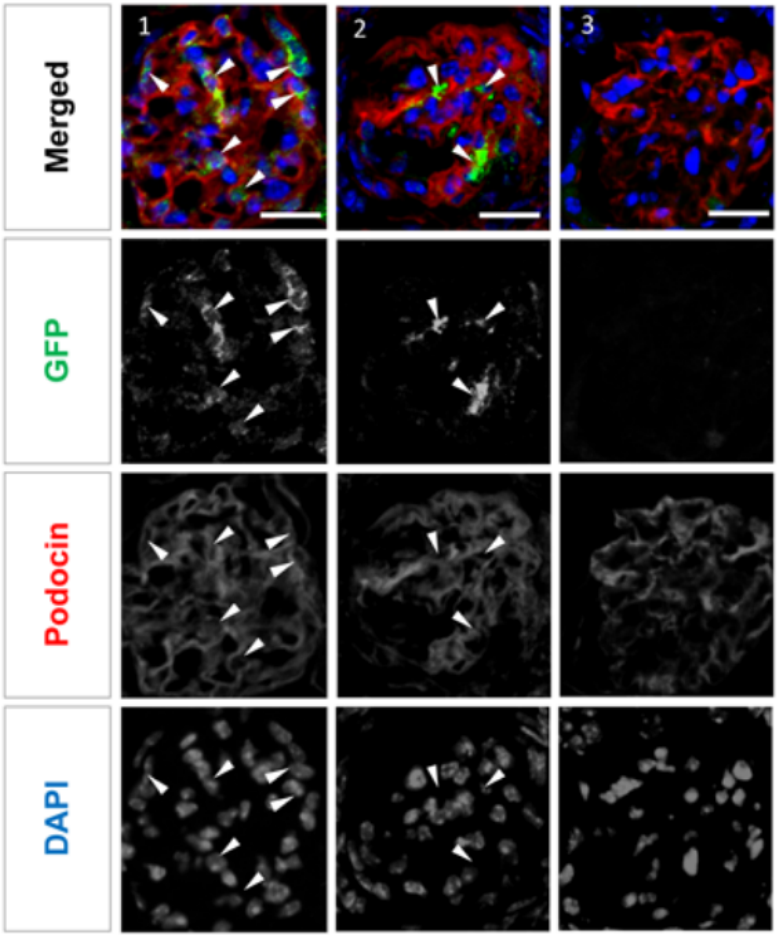

Supplementary Result 6

Single channel images used to produce Figure 2E.

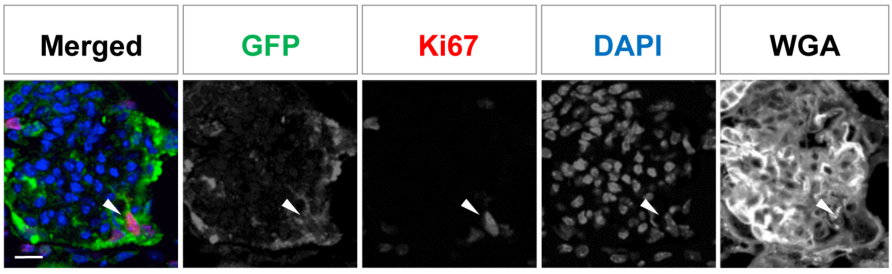

Supplementary Result 7

Single channel images used to produce Figure 3.

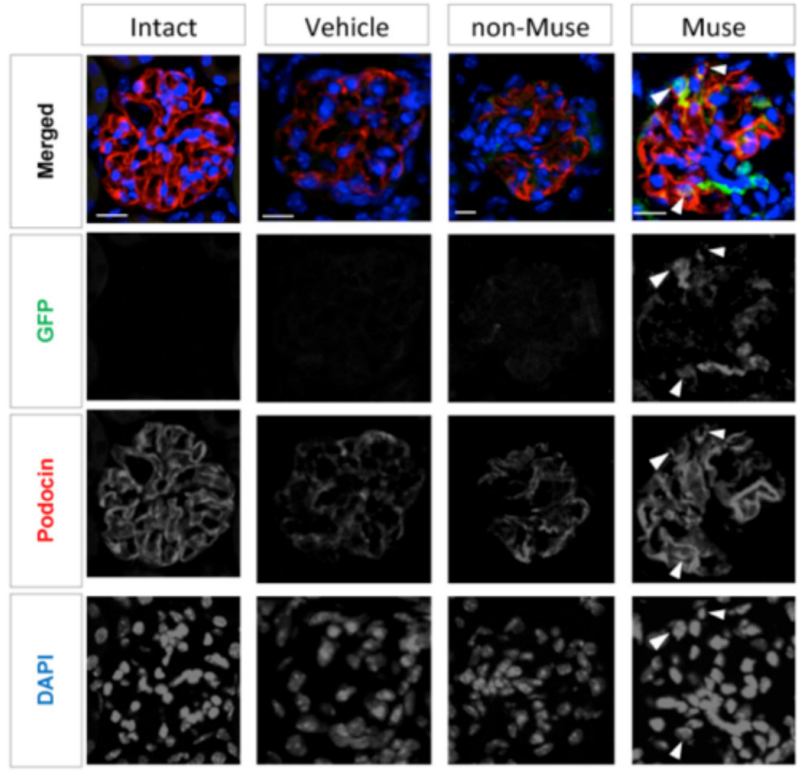

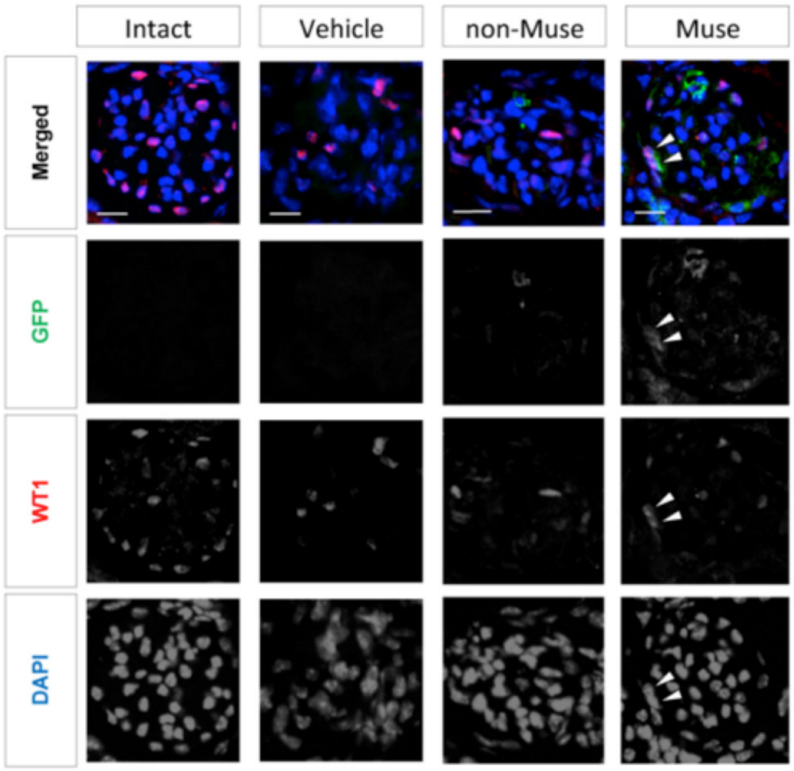

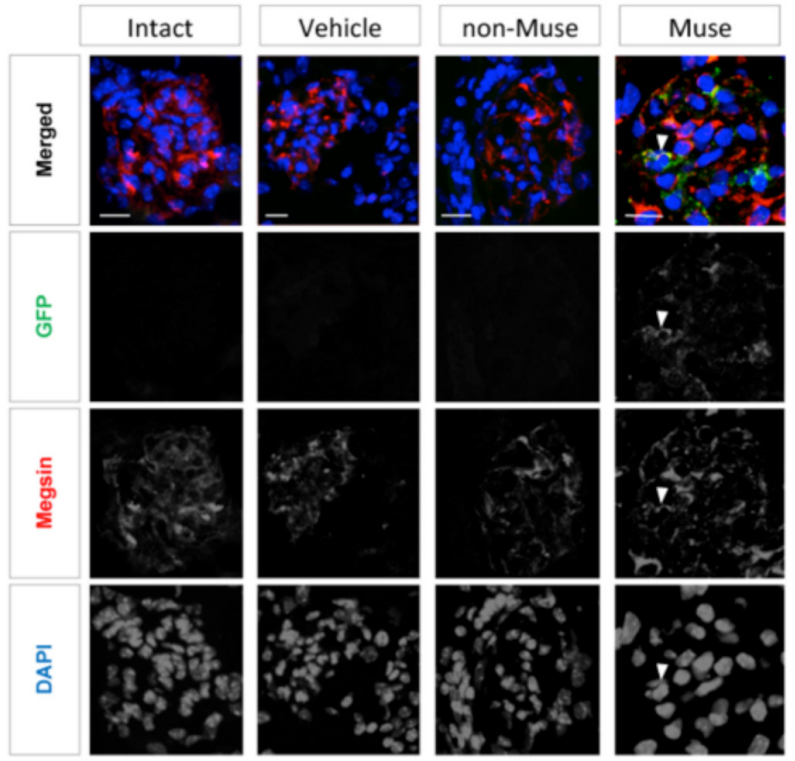
Intact
Vehicle
non-Muse
Muse
Merged
GFP
Megsin
DAPI

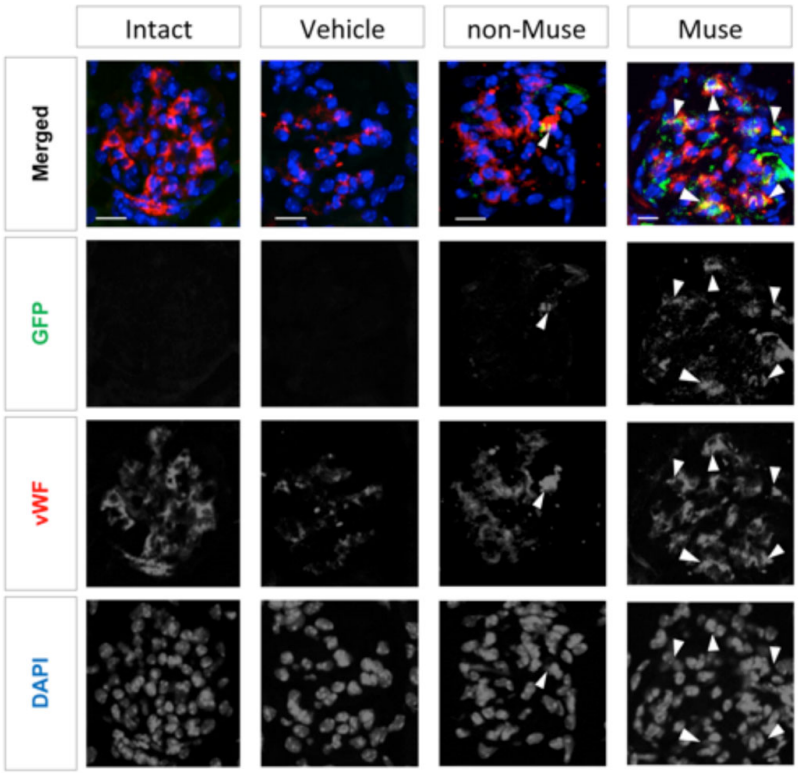
Intact
Vehicle
non-Muse
Muse
Merged
GFP
vWF
DAPI

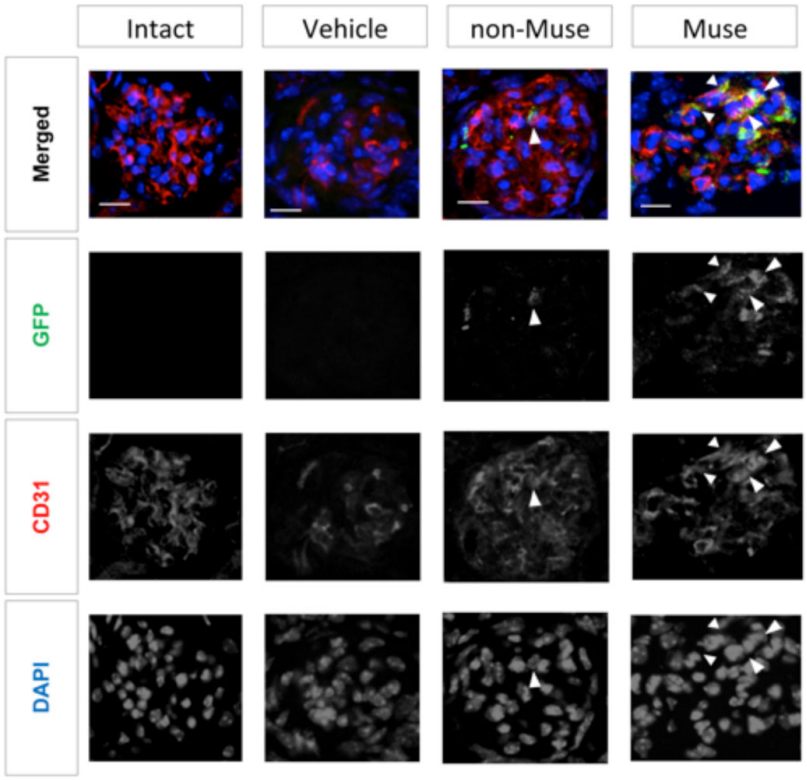
Intact
Vehicle
non-Muse
Muse
Merged
GFP
CD31
DAPI

Supplementary Result 8

Negative controls for immunohistochemistry

To assess the specificity of the primary antibodies, sections were stained only with secondary antibodies and then reacted with DAPI as the nuclear counterstain. Anti-rabbit IgG antibody conjugated to Alexa Fluor 568 was used for podocin, WT-1, megsin, vWF, and Ki67. Anti-goat IgG antibody conjugated to Alexa Fluor 568 and Alexa Fluor 680 were used for CD31. Anti-rat IgG antibody conjugated to Alexa Fluor 568 were used for CD45 and F4/80, and anti-goat IgG antibody and anti-rabbit IgG antibody conjugated to Alexa Fluor 488 were used for GFP and human Golgi complex, respectively. All the data for negative controls and target samples reacted with the primary and secondary antibodies were obtained under a laser confocal microscope using the same laser intensity and detection settings.

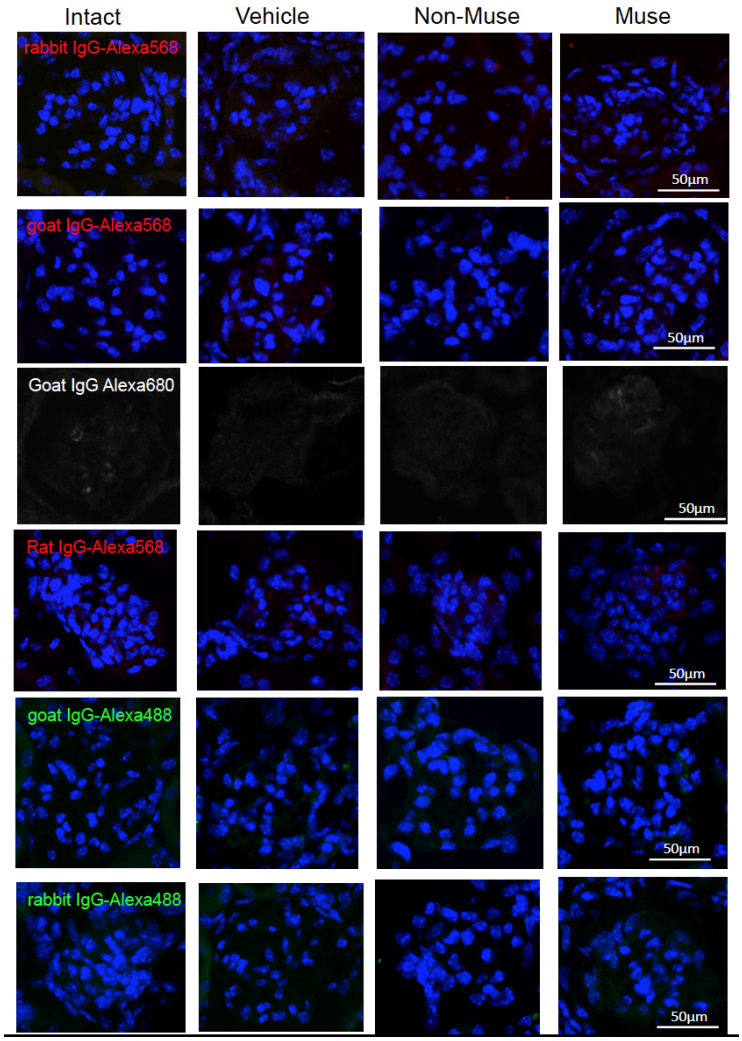

Supplementary Result 9

1) Interpretation of renal function

In our experiment, creatinine clearance was calculated based on the plasma creatinine and creatinine excretion in the urine.

Measurement of mouse creatinine clearance is generally inaccurate, because (1) the plasma creatinine level is so low that an automated analyzer for human creatinine cannot accurately measure the murine plasma creatinine concentration, and (2) efficient collection of urine is difficult because the volume of mouse urine is small. To address these issues, (1) we measured mouse creatinine using the QuantiChrom Creatinine Assay Kit (BioAssay Systems), which can detect plasma creatinine levels as low as 0.10 mg/dl, following the manufacturer's instructions, and (2) to minimize the uncertainty of creatinine excretion in the urine, we collected urine in a metabolic cage for 16 h. In addition, we dissolved dried urine on the floor of the metabolic cage with ultrapure water and collected it to the best of our ability. Total creatinine excretion was calculated from the creatinine concentration in the total amount of urine collected plus dissolved water to make the total volume ~5 ml.

While the plasma creatinine levels did not differ significantly among the Muse, non-Muse, and vehicle groups because of the narrow range of changes in the concentration, the urine creatinine excretion reflected differences in renal function. Creatinine clearance (= amount of creatinine discharge to urine/plasma creatinine concentration) was used to compare renal function between groups. Creatinine clearance was significantly different between the Muse and vehicle groups in FSGS-SCID mice (Figure 5), and between the Muse and vehicle and Muse and non-Muse groups in FSGS-BALB/c mice (Figure 7).

2) The mechanism of functional recovery in FSGS-SCID and FSGS -BALB/c:

SCID mice do not accurately reflect the pathology of human FSGS because FSGS progresses in combination with inflammatory cytokines and immune responses, which are deficient in SCID mice. Because the functional impairment was incomplete in the SCID model, the effect of Muse cells on functional recovery was not clear. In contrast to SCID mice, BALB/c mice, in which the immunologic system functions normally, could be used to generate a more complete kidney failure model and demonstrated that infused Muse cells could fully exert their reparative function. Therefore, the timing of inflammation and subsequent tissue damage, repair mechanisms, progression, and time course of renal failure and pathologic changes in SCID mice would all differ from those in BALB/c mice. This is one possible explanation for the difference in the extent of the recovery between the SCID and BALB/c FSGS models. Another possible explanation is the involvement of the immune system. The immune system normally exerts both positive and negative effects on tissue repair. When Muse cells were engrafted into FSGS-BALB/c glomeruli, the Muse cells might have replaced lost/damaged glomerular cells. They also appeared to exert trophic and

immunomodulatory effects based on the results of the mixed lymphocyte proliferation assay and expression of IDO with interferon-gamma licensing shown in Supplementary Result 10. These multiple actions could potentially lead to synergistic structural and functional regeneration of the glomerulus. SCID mice, however, lack the immune system that would be modified by the Muse cells. Cell replenishment alone could not generate a synergistic positive loop, and therefore the extent of recovery delivered by Muse cell infusion was not as high in SCID mice as in BALB/c mice.

Supplementary Result 10

Immunomodulatory effect of Muse cells

(A) Mixed lymphocyte proliferation assay; the presence of Muse and non-Muse cells inhibited the proliferation of T lymphocytes (p<0.001). (B) IDO activity assay and Western blot: neither Muse nor non-Muse cells constitutively expressed IDO, a mediator of MSC-immunosuppression. When stimulated with interferon-gamma, however, both Muse and non-Muse cells expressed IDO.

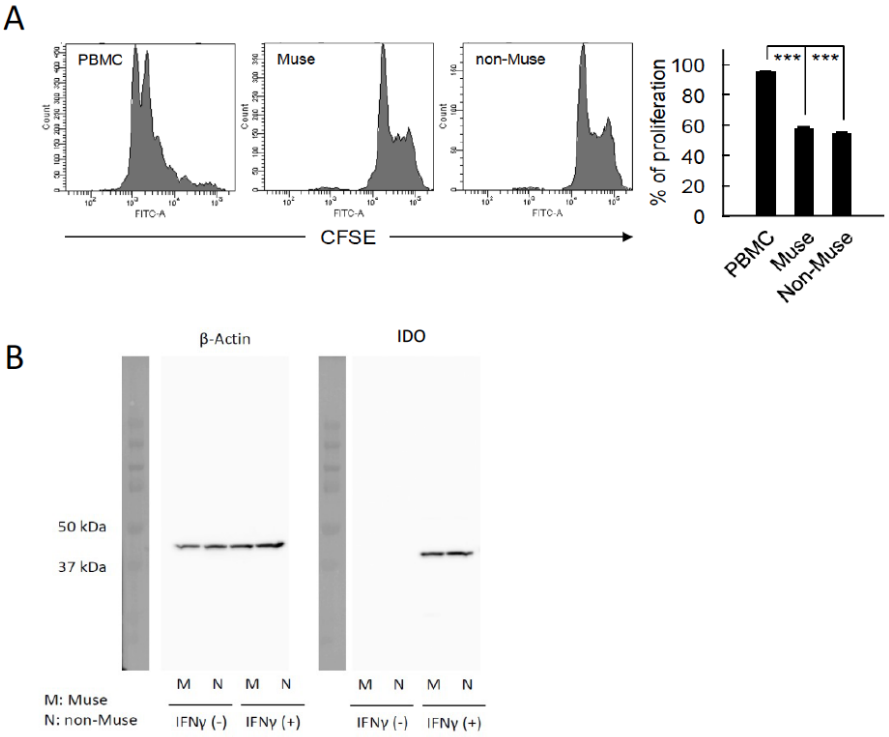

Supplementary Result 11

Glomerular marker expression in FSGS-BALB/c mice at 5 wk

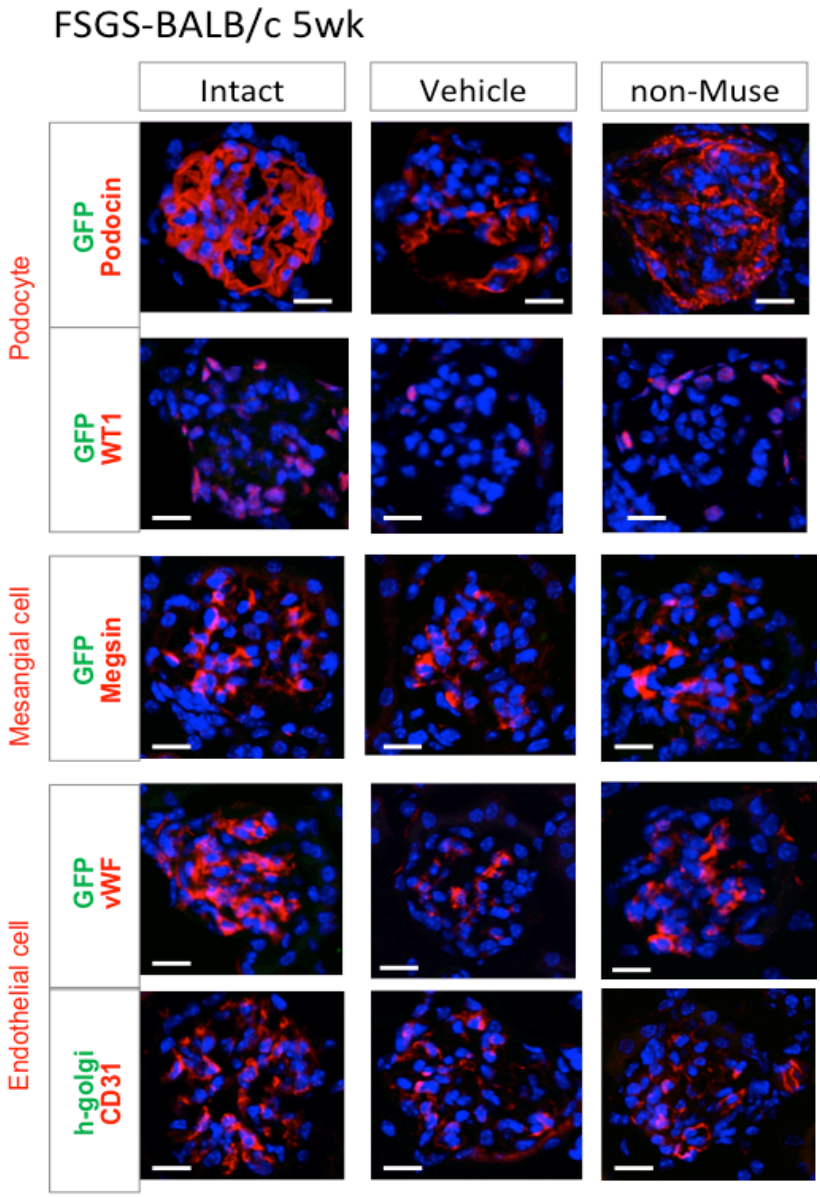

Because the intact and vehicle groups did not receive GFP(+) human Muse or non-Muse cell injection, GFP(+) or human Golgi complex (h-Golgi)(+) cells were not detected. In the non-Muse group, GFP(+) cells were hardly seen, probably due to immunorejection. Even in FSGS-SCID mice, very few human non-Muse cells were detected in the kidney at 2 wk. No immunosuppressant was administered to FSGS-BALB/c mice, and therefore non-Muse cells were considered to be rejected by 5 weeks. Bars = 20 μm.

Supplementary Result 12

Renoprotective effect of Muse cells.

FSGS-BALB/c mice were used for assessment of the renoprotective effects. TUNEL was performed in combination with podocin and CD31 immunohistochemistry at 3 d, 10 d, and 5 wk. The percent of TUNEL positivity in podocin- (A) and CD31-positive (B) cells in the glomerulus was significantly lower in the Muse group than in the vehicle group at 3 d ($p<0.05$) and the same tendency was still observed in podocin-positive cells at 10 d ($p<0.01$).

Proliferative activity in WT1-positive and CD31-positive cells was assessed either by PCNA (C) or Ki67 (D) at 3 d, 10 d, and 5 wk. At 10 d, the Muse group had the highest percentage of WT1(+)/PCNA(+) and Ki67(+)/CD31(+) cells among the three groups; a significantly higher percentage was recognized in the Muse group than in the vehicle and non-Muse groups for WT1(+)/PCNA(+) cells ($p<0.05$), and than in the vehicle group for Ki67(+)/CD31(+) cells ($p<0.05$). Podocin in A, WT1 in C, and CD31 in B and D were all detected by Alexa Fluor 647, and are shown as pseudo green-color coded.

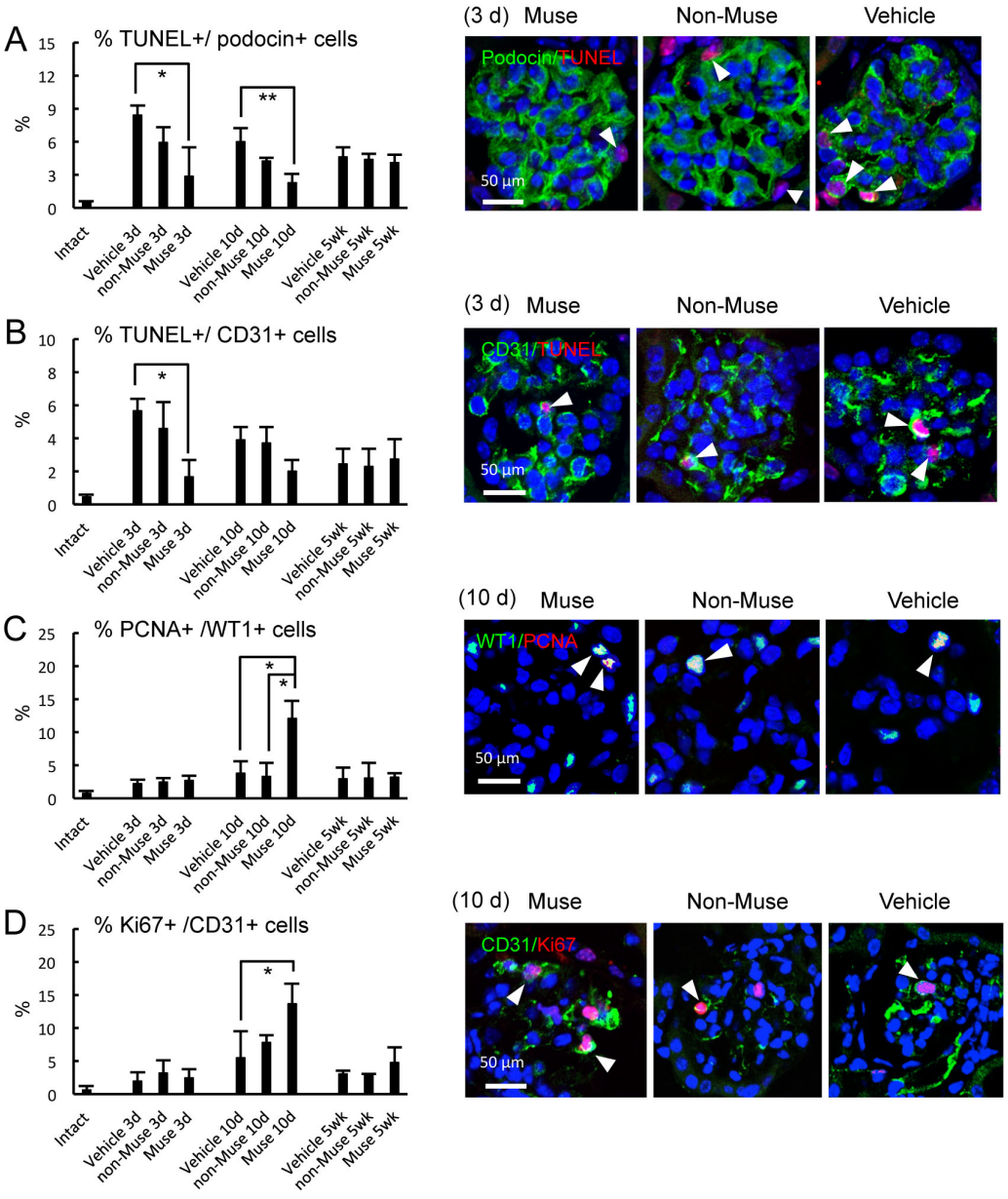
A
% TUNEL+/ podocin+ cells
%
15
12
9
6
3
0
*
**
Intact
Vehicle 3d
non-Muse 3d
Muse 3d
Vehicle 10d
non-Muse 10d
Muse 10d
Vehicle 5wk
non-Muse 5wk
Muse 5wk
B
% TUNEL+/ CD31+ cells
%
10
8
6
4
2
0
*
Intact
Vehicle 3d
non-Muse 3d
Muse 3d
Vehicle 10d
non-Muse 10d
Muse 10d
Vehicle 5wk
non-Muse 5wk
Muse 5wk
C
% PCNA+ /WT1+ cells
%
25
20
15
10
5
0
*
*
Intact
Vehicle 3d
non-Muse 3d
Muse 3d
Vehicle 10d
non-Muse 10d
Muse 10d
Vehicle 5wk
non-Muse 5wk
Muse 5wk
D
% Ki67+ /CD31+ cells
%
25
20
15
10
5
0
*
Intact
Vehicle 3d
non-Muse 3d
Muse 3d
Vehicle 10d
non-Muse 10d
Muse 10d
Vehicle 5wk
non-Muse 5wk
Muse 5wk
(3 d) Muse
Non-Muse
Vehicle
Podocin/TUNEL
50 μm
(3 d) Muse
Non-Muse
Vehicle
CD31/TUNEL
50 μm
(10 d) Muse
Non-Muse
Vehicle
WT1/PCNA
50 μm
(10 d) Muse
Non-Muse
Vehicle
CD31/Ki67
50 μm

Supplementary Result 13

Profile of renal regenerative growth factors in renal tissue of FSGS-SCID mice (2 wk)

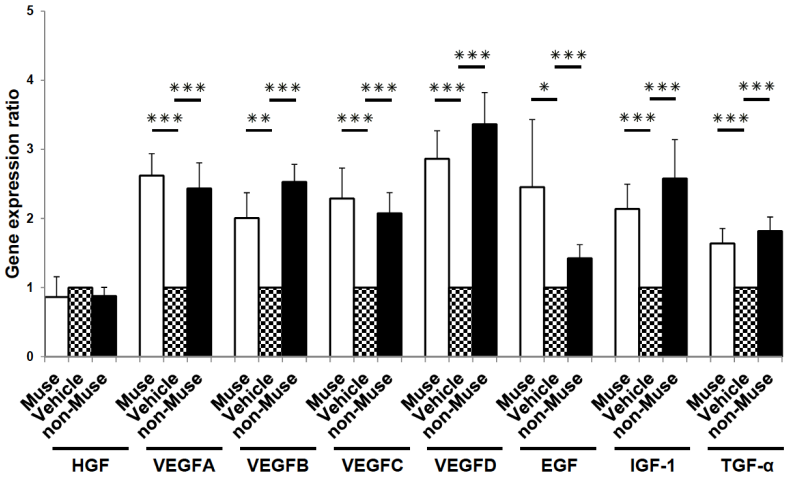

Samples of the FSGS-SCID mice kidney (2 wk) were subjected to Q-PCR to estimate the production activity of renal regenerative growth factors. Mouse primers were used to estimate the production level of endogenous renal cells. The Muse group had significantly higher gene expression levels of IGF-1, VEGF-A, VEGF-B, VEGF-C, VEGF-D, EGF, and TGF-alpha, which are involved in renoprotection,[12] than the vehicle group. The non-Muse group showed the same tendency as that of the Muse group and there was no significant difference between the two groups.

Supplementary Result 14

The ability of Muse cells to pass through the basement membrane

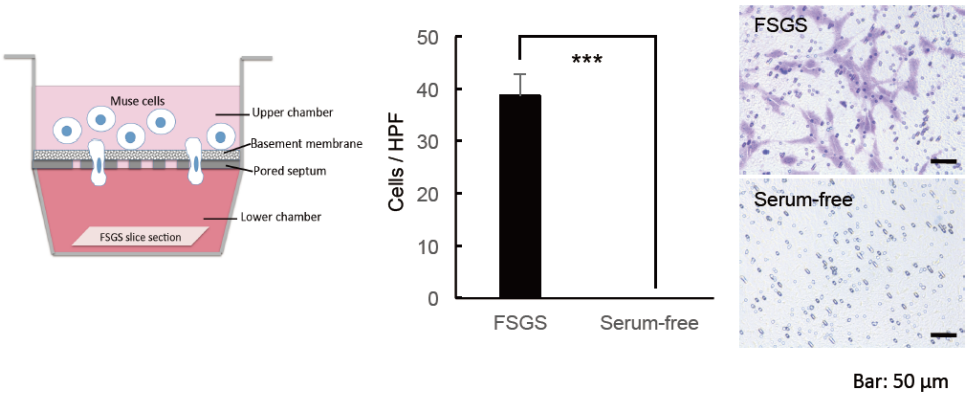

A CytoSelect 24-well Cell Invasion Assay, Colorimetric (Cell Biolabs Inc., San Diego, CA, CBA-110) was prepared. The upper surface of the microporous membrane located between the upper and lower chambers was coated with a uniform layer of basement membrane matrix (Cell Biolabs). Muse cells with serum-free media were placed in the upper chamber, and a slice of

FSGS-SCID kidney (FSGS) was placed in the lower chamber. For the control, serum-free medium was placed in the lower chamber. The number of Muse cells that migrated into the lower chamber through the basement membrane matrix was calculated 24 h after incubation. No migrated cells were observed in the serum-free media, whereas the migration of 38.7±4.2 cells/high power field (HPF; using 20X objective lens) was observed when the FSGS-SCID kidney slice was placed in the chamber. Based on the fact that Muse cells produce MMP-1, -2, and -9, which degrade the matrix,[11] Muse cells are suggested to be able to pass through the basement membrane.

It is possible that podocyte loss causes a focal structural slacking and/or micro-disruption of the glomerular basement membrane (GBM) that creates a path for migrating Muse cells. The GBM is a dynamic, rather than static, structure. While GBM turnover exceeds 100 d in the normal adult rat glomerulus,[13] GBM turnover is accelerated under pathologic conditions such as renal failure.[14] Podocytes play a central role in GBM turnover and prevent the disruption of vessels by physically protecting the vessels from transcapillary pressure. If podocytes are lost, an imbalance of GBM generation/degradation may be triggered in the corresponding focal area, allowing for excessive tension, serum leakage, and micro-disruption of the GBM.[15] Micro-disruption could provide a path for the migration of Muse cells.

Under pathologic conditions, particularly when podocytes are damaged or lost, the GBM may be microscopically damaged. These mechanisms could potentially underlie the migration of Muse cells out of the capillary, passing through the GBM, and penetrating into the glomerulus.

References

1. Kuroda, Y, Wakao, S, Kitada, M, Murakami, T, Nojima, M, Dezawa, M: Isolation, culture and evaluation of multilineage-differentiating stress-enduring (Muse) cells. *Nat Protoc* 8: 1391-1415, 2013.
2. Nguyen, TH, Khakhoulina, T, Simmons, A, Morel, P, Trono, D: A simple and highly effective method for the stable transduction of uncultured porcine hepatocytes using lentiviral vector. *Cell Transplant* 14: 489-496, 2005.
3. Shimizu, S, Kitada, M, Ishikawa, H, Itokazu, Y, Wakao, S, Dezawa, M: Peripheral nerve regeneration by the in vitro differentiated-human bone marrow stromal cells with Schwann cell property. *Biochem Biophys Res Commun* 359: 915-920, 2007.
4. Batchelder, CA, Lee, CC, Matsell, DG, Yoder, MC, Tarantal, AF: Renal ontogeny in the rhesus monkey (Macaca mulatta) and directed differentiation of human embryonic stem cells towards kidney precursors. *Differentiation* 78: 45-56, 2009.
5. Alcoser, SY, Kimmel, DJ, Borgel, SD, Carter, JP, Dougherty, KM, Hollingshead, MG: Real-time PCR-based assay to quantify the relative amount of human and mouse tissue present in tumor xenografts. *BMC Biotechnol* 11: 124, 2011.
6. Iseki, M, Kushida, Y, Wakao, S, Akimoto, T, Mizuma, M, Motoi, F, Asada, R, Shimizu, S, Unno, M, Chazenbalk, G, Dezawa, M: Human Muse cells, non-tumorigenic pluripotent-like stem cells, have the capacity for liver regeneration by specific homing and replenishment of new hepatocytes in liver fibrosis mouse model. *Cell Transplant* doi: 10.3727/096368916X693662., 2016.
7. Chinnadurai, R, Copland, IB, Patel, SR, Galipeau, J: IDO-independent suppression of T cell effector function by IFN-gamma-licensed human mesenchymal stromal cells. *J Immunol* 192: 1491-1501, 2014.
8. Lee, VW, Harris, DC: Adriamycin nephropathy: a model of focal segmental glomerulosclerosis. *Nephrology (Carlton)* 16: 30-38, 2011.
9. Kuroda, Y, Kitada, M, Wakao, S, Nishikawa, K, Tanimura, Y, Makinoshima, H, Goda, M, Akashi, H, Inutsuka, A, Niwa, A, Shigemoto, T, Nabeshima, Y, Nakahata, T, Nabeshima, Y, Fujiyoshi, Y, Dezawa, M: Unique multipotent cells in adult human mesenchymal cell populations. *Proc Natl Acad Sci U S A* 107: 8639-8643, 2010.
10. Katagiri, H, Kushida, Y, Nojima, M, Kuroda, Y, Wakao, S, Ishida, K, Endo, F, Kume, K, Takahara, T, Nitta, H, Tsuda, H, Dezawa, M, Nishizuka, SS: A distinct subpopulation of bone marrow mesenchymal stem cells, Muse cells, directly commit to the replacement of liver components. *Am J Transplant* 16: 468-483, 2016.
11. Iseki, M, Kushida, Y, Wakao, S, Akimoto, T, Mizuma, M, Motoi, F, Asada, R, Shimizu, S, Unno, M, Chazenbalk, G, Dezawa, M: Human Muse cells,

non-tumorigenic pluripotent-like stem cells, have the capacity for liver regeneration by specific homing and replenishment of new hepatocytes in liver fibrosis mouse model. *Cell Transplant* doi: 10.3727/096368916X693662, 2016.

12. Ezquer, ME, Ezquer, FE, Arango-Rodriguez, ML, Conget, PA: MSC transplantation: a promising therapeutic strategy to manage the onset and progression of diabetic nephropathy. *Biol Res* 45: 289-296, 2012.
13. Price, RG, Spiro, RG: Studies on the metabolism of the renal glomerular basement membrane. Turnover measurements in the rat with the use of radiolabeled amino acids. *J Biol Chem* 252: 8597-8602, 1977.
14. Marshall, CB: Rethinking glomerular basement membrane thickening in diabetic nephropathy: adaptive or pathogenic? *Am J Physiol Renal Physiol* 311: F831-F843, 2016.
15. Nagata, M: Podocyte injury and its consequences. *Kidney Int* 89: 1221-1230, 2016.